Commun. Comput. Phys.
doi: 10.4208/cicp.OA-2015-0001

Vol. **20**, No. 3, pp. 689-702
September 2016

Field-Free Molecular Orientation Induced by a Single-Cycle THz Laser Pulse Train

Xiao-Miao Zhang, Jian Li, Jie Yu* and Shu-Lin Cong

School of Physics and Optoelectronic Technology, Dalian University of Technology, Dalian 116024, China.

Communicated by Michel A. Van Hove

Received 27 October 2015; Accepted (in revised version) 28 January 2016

Abstract. We investigate theoretically the field-free orientation of CO molecules induced by a single-cycle THz laser pulse train. It is shown that the molecular orientation can be obviously enhanced by applying the pulse train. The laser intensity and pulse number have some effects on the molecular orientation. The high degree of field-free molecular orientation $|\langle\cos\theta\rangle|_{\max}=0.9246$ is obtained at temperature $T=0$ K. The variations of the maximum orientation degree with the experimentally available pulse number and peak intensity are given. Temperature T has a considerable influence on the field-free molecular orientation. The maximal field-free molecular orientation at $T=0$, 10, 20 and 30 K for $N=14$ and $E_0=1.8$ MV/cm are $|\langle\cos\theta\rangle|_{\max}=0.9188$, 0.7338, 0.6055 and 0.5154 in order, and the corresponding effective duration times of molecular orientation are $\Delta t=0.759$, 0.432, 0.297 and 0.117 ps.

PACS: 34.50.Rk, 82.20.Bc, 82.50.Nd, 82.30.Nr

Key words: Single-cycle THz laser pulse train, pulse number, molecular orientation.

1 Introduction

Molecular alignment and orientation have drawn substantial attention of both physicists and chemists in the past few decades due to their extensive applications in relevant research fields [1, 2], such as high-order harmonic generation [3–6], chemical reaction dynamics [7–11], strong-field ionization [12], ultrafast molecular imaging [13–15] and attosecond science [16]. Alignment implies that the symmetry axis of molecule is localized along a laboratory-fixed axis (the polarization direction of the laser field), and orientation additionally requires the aligned molecules point along a particular direction. The

*Corresponding author. *Email addresses:* xiaomiaozhang@mail.dlut.edu.cn (X.-M. Zhang), dlut_lijian@mail.dlut.edu.cn (J. Li), yujie@dlut.edu.cn (J. Yu), shlcong@dlut.edu.cn (S.-L. Cong)

 ©2016 Global-Science Press

https://doi.org/10.4208/cicp.OA-2015-0001 Published online by Cambridge University Press

molecular alignment has been realized experimentally [17–21]. However, the realization of molecular orientation is still a challenging issue.

Several ways have been proposed to manipulate molecular orientation. Originally, a strong dc-field, such as a hexapole field [22] or brute forced field [23], based on its interaction with the permanent dipole moment, was employed to achieve molecular orientation. However, this way can only obtain relatively low orientation degree, and strong dc-field often induces the stark effects influencing the experimental measurement. Alternatively, Friedrich *et al*. proposed a scheme for enhancing the molecular orientation by an intense laser field combined with a weak dc-field. The effectiveness of this scheme depends on the combined effects of the permanent dipole interaction and the anisotropic polarizability interaction [24, 25]. The maximal degree of molecular orientation achieved by using this scheme was greatly improved. However, the presence of an electric field may perturb the quantum states of the target molecule and limit applications of the oriented samples [26]. Additionally, an asymmetric laser field, such as a half-cycle pulse (HCP) [27–29], a few-cycle THz laser field [30, 31], a two-color laser field [32–36] and a multi-color laser field [37], was employed to steer molecular orientation via their interaction with molecular permanent dipole moment, anisotropic polarizability and hyperpolarizability. These ways can be used to realize effectively field-free molecular orientation. In experiment, however, it is difficult to generate intense HCPs at present. Moreover, the intense two-color or multi-color ultrafast laser fields potentially cause unwanted molecular excitations leading to molecular ionization or dissociation. Resulting from the recent breakthrough in THz technology, the intense single-cycle THz pulses have become available in the laboratory [38]. Kitano *et al*. obtained theoretically a high degree of field-free orientation of $\langle\cos\theta\rangle$=0.84 in the HBr molecule by the combination of a femtosecond laser field and a time-delayed single-cycle THz laser pulse [26]. In their scheme, a nonresonant femtosecond laser pulse was used to pre-excite molecules and a time-delayed THz pulse was used to orient molecules. After the nonresonant femtosecond laser pulse is over, the even rotational states are populated and the molecule sample is aligned. The transition frequency becomes resonant with the subsequent THz pulse after pre-excitation, the molecules can be consequently oriented. Fleischer *et al*. measured the field-free molecular orientation induced by an intense single-cycle THz laser pulse in the OCS gas sample [39]. Theoretically, single-cycle THz pulses was utilized to realize orientation of the HCN molecule [40].

In the present work, we investigate theoretically the efficient field-free molecular orientation steered by a single-cycle THz laser pulse train. We study the influence of the laser intensity and pulse number on the maximum orientation degree. We find that the nearly equal populations on neighboring rotational states can lead to a large orientation degree. The optimal pulse number in the range of peak intensity of E_0=[0.1,10.1] MV/cm are given. The influences of temperature on molecular orientation degree and duration time are discussed.

https://doi.org/10.4208/cicp.OA-2015-0001 Published online by Cambridge University Press

2 Theoretical calculation methods

In our scheme, a single-cycle THz pulse train is employed to steer field-free orientation of the CO molecule, based on its interaction with molecular permanent dipole moment. Owing to the small permanent dipole moment of the CO molecule and low peak intensity of THz pulse, the permanent dipole interaction is weak. The single-cycle THz pulse induces resonant dipole transition between the even and odd rotational states according to the selection rule of $\Delta J=\pm 1$ and $\Delta M=0$. The CO molecule is excited from the $J=0$ state to higher $J\geq 2$ states continuously by a THz pulse train, in order to guarantee that more rotational states can be populated and a large orientation degree can be obtained. The electric field of single-cycle THz pulse train is expressed as [41]

$$E_{\mathtt{THz}}(t)=\sum_{j=1}^{N}E_j(t)=\sum_{j=1}^{N}E_{0j}f_j(t)/E_{\mathtt{peak}}, \tag{2.1}$$

with

$$f_j(t)=\exp(-2\ln 2(t-t_{\mathtt{p}_j})^2/\tau_j^2)\cos[\omega_j(t-t_{\mathtt{p}_j})+\phi_j], \tag{2.2}$$

$$E_{\mathtt{peak}}=|f_j(t)|_{\max}, \tag{2.3}$$

where E_{0j}, $t_{\mathtt{p}_j}$, τ_j, ω_j and ϕ_j are the peak intensity, central time, full width at half maximum (FWHM), central frequency and carrier envelope phase of the jth THz pulse in order. In our calculation, for simplicity, we set $E_{0j}=E_0$, $t_{\mathtt{p}_j}=jt_d$, $\tau_j=\tau$, $\omega_j=\omega$ and $\phi_j=\phi$, where t_d is the delay time between two neighboring pulses. Within the rigid rotor approximation, the Hamiltonian of the CO molecule irradiated by the single-cycle THz pulse train is given by [41]

$$\hat{H}(t)=B_e\hat{J}^2-\mu E_{\mathtt{THz}}(t)\cos\theta, \tag{2.4}$$

where the first term is the molecular rotational energy and the second term is the dipole interaction between the single-cycle THz pulse train and molecular permanent dipole moment. B_e, $\hat{J}$ and μ are the molecular rotational constant, angular momentum operator and permanent dipole moment in order. θ is the angle between the molecular axis and the polarization direction of the laser field. The degree of molecular orientation is calculated by

$$\langle\cos\theta\rangle=\mathbf{Tr}\{\cos\theta\hat{\rho}(t)\}, \tag{2.5}$$

where **Tr** denotes a trace and $\hat{\rho}(t)$ is the time-dependent density operator. The time evolution of the density operator can be obtained by solving the quantum Liouville equation,

$$\frac{d\hat{\rho}(t)}{dt}=-\frac{i}{\hbar}[\hat{H},\hat{\rho}(t)]. \tag{2.6}$$

https://doi.org/10.4208/cicp.OA-2015-0001 Published online by Cambridge University Press

The density operator can be expanded in the eigenstates of the rigid rotor Hamiltonian as [42]

$$\hat{\rho}(t)=\sum_{J,M,J',M'}\rho_{JMJ'M'}(t)|JM\rangle\langle J'M'|, \tag{2.7}$$

where the matrix elements of the density operator $\rho_{JMJ'M'}(t)$ are determined by coupling differential equations [43]

$$\begin{aligned}\frac{d\rho_{JMJ'M'}(t)}{dt}&=-\frac{i}{\hbar}[\hat{H}\hat{\rho}(t)-\hat{\rho}(t)\hat{H}]_{JMJ'M'}\\&=-\frac{i}{\hbar}\left\{\sum_{J_1M_1}\langle JM|B_e\hat{J}^2|J_1M_1\rangle\rho_{J_1M_1J'M'}(t)-\sum_{J_1M_1}\langle J_1M_1|B_e\hat{J}^2|J'M'\rangle\rho_{JMJ_1M_1}(t)\right\}\\&\quad+\frac{i}{\hbar}\mu E_{\mathrm{THz}}(t)\left\{\sum_{J_1M_1}\langle JM|\cos\theta|J_1M_1\rangle\rho_{J_1M_1J'M'}(t)\right.\\&\quad\left.-\sum_{J_1M_1}\langle J_1M_1|\cos\theta|J'M'\rangle\rho_{JMJ_1M_1}(t)\right\}\\&=-\frac{i}{\hbar}(\varepsilon_J-\varepsilon_{J'})\rho_{JMJ'M'}(t)\\&\quad+\frac{i}{\hbar}\mu E_{\mathrm{THz}}(t)\sum_{J_1M_1}\left\{V^{(1)}_{JMJ_1M_1}\rho_{J_1M_1J'M'}(t)-V^{(1)}_{J_1M_1J'M'}\rho_{JMJ_1M_1}(t)\right\},\end{aligned} \tag{2.8}$$

where $V^{(1)}_{JMJ'M'}=\langle JM|\cos\theta|J'M'\rangle$, and $\varepsilon_J=B_eJ(J+1)$ is the molecular energy in the $|JM\rangle$ state. We solve numerically the above equations by using the fourth-order Runge-Kutta method.

Under the action of linearly polarized THz pulses, the magnetic quantum number of the CO molecule remains unchanged. For simplicity, the magnetic quantum number is taken to be $M=0$. At temperature $T=0$ K, the initial state $|JM\rangle_{init}$ is the ground rotational state $|0,0\rangle$. The time-dependent density operator is given by

$$\hat{\rho}(t)=|\Psi(t)\rangle\langle\Psi(t)|, \tag{2.9}$$

with

$$|\Psi(t)\rangle=\sum_{J=0}^{\infty}C_{J,M}(t)|J,M\rangle\exp(-i\varepsilon_Jt/\hbar), \tag{2.10}$$

where $C_{J,M}(t)$ is a complex number. The molecular orientation degree can be written as

$$\begin{aligned}\langle\cos\theta\rangle(t)&=\sum_{J,M,J',M'}\langle JM|\hat{\rho}(t)|J'M'\rangle\langle J'M'|\cos\theta|JM\rangle\\&=\sum_{J,M,J',M'}|C_{JM}(t)||C_{J'M'}(t)|V^{(1)}_{J'M'JM}\times\cos[(\varepsilon_J-\varepsilon_{J'})t/\hbar-(\varphi_J-\varphi_{J'})]\\&=2\sum_{J=0}^{\infty}|C_{J+1,M}(t)||C_{J,M}(t)|V^{(1)}_{J+1,M,J,M}\times\cos(\Delta E_{J+1,J}t/\hbar-\Delta\varphi_{J+1,J}),\end{aligned} \tag{2.11}$$

https://doi.org/10.4208/cicp.OA-2015-0001 Published online by Cambridge University Press

with $|C_{JM}(t)|=|\rho_{JMJM}(t)|$ and $|C_{J'M'}(t)|=|\rho_{J'M'J'M'}(t)|$.

At temperature $T\neq 0$ K, different rotational states are incoherently populated, and the initial density operator satisfies the temperature-dependent Boltzmann distribution:

$$\rho_0(T)=\frac{1}{Z}\sum_{J=0}^{\infty}\sum_{M=-J}^{M=J}|JM\rangle\langle JM|\exp[-B_eJ(J+1)/\kappa_BT], \tag{2.12}$$

where

$$Z=\sum_{J=0}^{\infty}\sum_{M=-J}^{M=J}\exp[-B_eJ(J+1)/\kappa_BT] \tag{2.13}$$

is the partition function with the Boltzmann constant κ_B at temperature T. The molecular orientation degree can be written as

$$\begin{aligned}\langle\langle\cos\theta\rangle\rangle(t)=&\sum_{J_{init}=0}^{\infty}\frac{1}{Z}\exp[-B_eJ_{init}(J_{init}+1)/\kappa_BT]\\&\times\sum_{M_{init}=-J_{init}}^{J_{init}}\langle\cos\theta\rangle_{J_{init},M_{init}}(t).\end{aligned} \tag{2.14}$$

3 Results and discussions

In our calculation, the rotational constant $B_e=1.93$ cm^{-1} and permanent dipole moment $\mu=0.112$ D of the CO molecule are obtained from Ref. [37]. The parameters of single-cycle THz pulses are taken to be $\tau=1.0$ ps, $\omega=0.5$ THz, $\phi=1.5\,\pi$ and $t_{\mathrm{p}_j}=jt_d$. Here, the delay time between two neighboring THz pulses is optimized to be $t_d=8.62$ ps. We firstly investigate the molecular orientation dynamics at temperature $T=0$ K. According to the Maxwell equation, the electric field must satisfy the condition of $\int E(t)dt=0$ [31]. The time evolution of a single-cycle THz pulse meets this integral condition, as shown in Fig. 1(a). It can be seen from Fig. 1(b) that the molecular orientation and alignment can be achieved after the THz pulse is over, and the field-free molecular orientation repeatedly revives at $t=nT_{rot}$ $(n=0,1,2,\cdots)$, where $T_{rot}=h/2B_e=8.64$ ps is the rotational period of the CO molecule. The maximum orientation degree and alignment degree induced by a single-cycle THz pulse with $E_0=1.1$ MV/cm are $|\langle\cos\theta\rangle|_{\max}=0.0732$ and $\langle\cos^2\theta\rangle_{\max}=0.3372$ in Fig. 1(b). When a single-cycle THz pulse train with E_0=1.1 MV/cm and N=20 is used, we obtain $|\langle\cos\theta\rangle|_{\max}=0.8977$ and $\langle\cos^2\theta\rangle_{\max}=0.8510$. The molecular orientation and alignment steered by a single-cycle THz pulse train are obviously enhanced. The variations of maximum orientation degree with the peak intensity E_0 and pulse number N of the THz pulse train are shown in Fig. 1(d). When $E_0\leq 1.2$ MV/cm, the maximal molecular orientation degree increases slowly and monotonously with the increase of pulse number. When $E_0>1.2$ MV/cm, the maximum orientation degree firstly increases

https://doi.org/10.4208/cicp.OA-2015-0001 Published online by Cambridge University Press

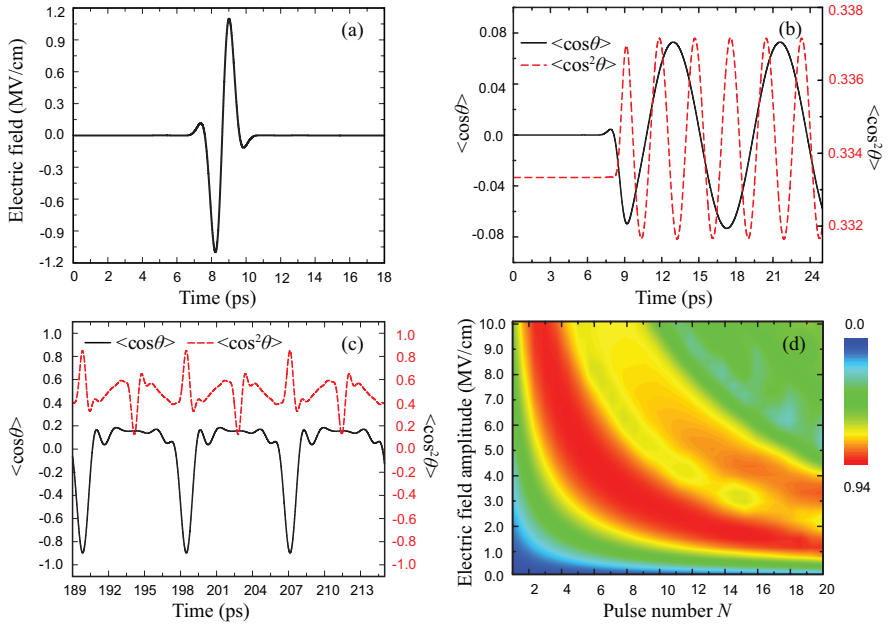


Figure 1: (a) The time evolution of a single-cycle THz pulse with $E_0=1.1$ MV/cm, $t_p=t_d=8.62$ ps, $\tau=1.0$ ps, $\omega=0.5$ THz and $\phi=1.5\pi$. (b) The time evolutions of the molecular orientation (solid black line) and alignment (dash red line) steered by a single-cycle THz pulse for $E_0=1.1$ MV/cm. (c) The time evolutions of the molecular orientation (solid black line) and alignment (dash red line) steered by a single-cycle THz pulse train for $E_0=1.1$ MV/cm and $N=20$. (d) The variation of $|\langle\cos\theta\rangle|_{\max}$ with the electric-field amplitude E_0 and pulse number N.

with the pulse number, then decreases and oscillates. On the other hand, $|\langle\cos\theta\rangle|_{\max}$ has a monotonous growth by increasing the peak intensity from $E_0=0.1$ to 10.1 MV/cm for $N=1$ and 2. When $N\geq 3$, $|\langle\cos\theta\rangle|_{\max}$ oscillates with the increase of peak intensity. By changing the peak intensity and pulse number of the THz pulse train, the maximum orientation degree can be lowered or enhanced. We elaborate the variations of $|\langle\cos\theta\rangle|_{\max}$ in the following discussion.

Firstly, we take $E_0=0.1$, 0.5, 1.1 and 1.2 MV/cm as examples to illustrate the variations of $|\langle\cos\theta\rangle|_{\max}$ as a function of the pulse number. As shown in Fig. 2(a), $|\langle\cos\theta\rangle|_{\max}$ linearly increases for $E_0=0.1$ and 0.5 MV/cm from 0.0067 to 0.1323 and from 0.0334 to 0.5879, respectively. When $E_0=1.1$ and 1.2 MV/cm, $|\langle\cos\theta\rangle|_{\max}$ increases rapidly by adding pulse number from $N=1$ to 16, and increases lightly when $N\geq 17$. The time evolution of molecular orientation induced by a single-cycle THz pulse train for $N=5$ and $E_0=0.1$ MV/cm is shown in Fig. 2(b). The maximal field-free molecular orientation degree is enhanced gradually during the action of the THz pulse train. The final maximum orientation degree is 0.0333. When the pulse number increases from $N=5$ to 20, a larger maximum orientation degree $|\langle\cos\theta\rangle|_{\max}=0.1323$ is obtained. It can be seen in Fig. 2(c) that only the rotational states $|0,0\rangle$ and $|1,0\rangle$ are populated for $N=1$ and $E_0=0.1$ MV/cm. Owing to the weak interaction between the electric field and permanent dipole moment,

https://doi.org/10.4208/cicp.OA-2015-0001 Published online by Cambridge University Press

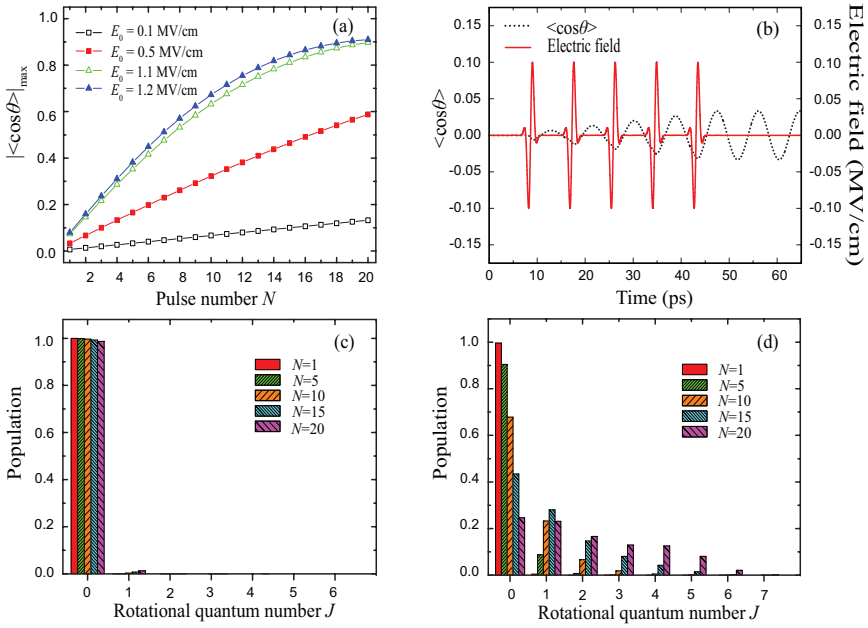


Figure 2: (a) The maximal orientation degree $|\langle\cos\theta\rangle|_{\max}$ as a function of the pulse number N for $E=0.1$ MV/cm (black open-square line), 0.5 MV/cm (red solid-square line), 1.1 MV/cm (green open-triangle line) and 1.2 MV/cm (blue solid-triangle line). (b) The time evolution of molecular orientation induced by a single-cycle THz pulse train with $E_0=0.1$ MV/cm and $N=5$. (c) The rotational population distributions at $N=1$ (red bar), 5 (green bar), 10 (orange bar), 15 (cyan bar) and 20 (magenta bar) for $E_0=0.1$ MV/cm. (d) The rotational population distributions at $N=1$ (red bar), 5 (green bar), 10 (orange bar), 15 (cyan bar) and 20 (magenta bar) for $E_0=1.1$ MV/cm.

when N=5, 10, 15 and 20, the populations on the rotational states $|1,0\rangle$ and $|2,0\rangle$ are much smaller than that on the $|0,0\rangle$ state. As a result, the corresponding maximum orientation degrees are very small. In Fig. 2(d), when $E_0=1.1$ MV/cm and $N=1$, the populations on the rotational states $|0,0\rangle$ and $|1,0\rangle$ are $P_{0,0}=0.99997$ and $P_{1,0}=0.3\times10^{-4}$, respectively. The corresponding maximum orientation degree is $|\langle\cos\theta\rangle|_{\max}=0.0732$. When $N=5$, the highest populated rotational state is $|2,0\rangle$, and $|\langle\cos\theta\rangle|_{\max}=0.3525$. When $N=10$, 15 and 20, the highest populated rotational states are $|4,0\rangle$, $|6,0\rangle$ and $|7,0\rangle$ in order. With the increase of pulse number, there are more rotational states being excited. When $E_0=1.1$ MV/cm, the maximum orientation degrees for $N=10$, 15 and 20 are $|\langle\cos\theta\rangle|_{\max}=0.6323$, 0.8111 and 0.8977, respectively. In short, when the peak intensity lies in the range of $E_0=[0.1,1.2]$ MV/cm, $|\langle\cos\theta\rangle|_{\max}$ increases continuously with the increase of pulse number from $N=1$ to 20.

The resonant dipole transitions from the $J=0$ to $J\geq2$ states are restricted by the selection rule of $\triangle J=\pm1$ and the weak interaction between the laser field and permanent dipole moment when the electric-field intensity varies in the range of $E_0=[0.1,1.2]$ MV/cm. In this case, only the $|0,0\rangle$ and $|1,0\rangle$ states are populated, and the population on the $|0,0\rangle$ state is much larger than that on the $|1,0\rangle$ state. According to Eq. (2.11),

https://doi.org/10.4208/cicp.OA-2015-0001 Published online by Cambridge University Press

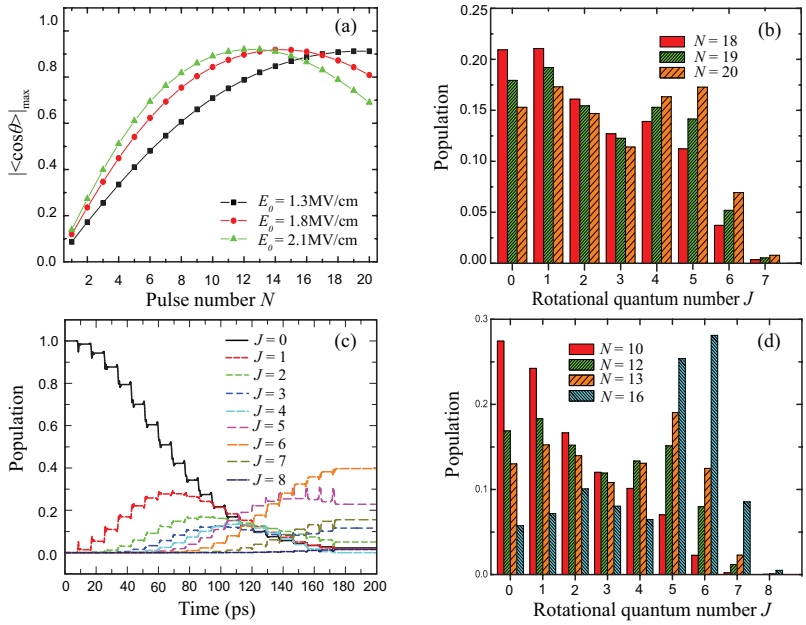


Figure 3: (a) The maximal orientation degree $|\langle\cos\theta\rangle|_{\max}$ as a function of the pulse number N for $E_0=1.3$ MV/cm (black solid-square line), 1.8 MV/cm (red solid-circle line) and 2.1 MV/cm (green solid-triangle line). (b) The rotational population distributions at $N=18$ (red bar), 19 (green bar) and 20 (orange bar) for $E_0=1.3$ MV/cm. (c) The time evolution of populations on the $J=0$–8 states for $N=20$ and $E_0=2.1$ MV/cm. (d) The rotational population distributions at $N=10$ (red bar), 12 (green bar), 13 (orange bar) and 16 (cyan bar) for $E_0=2.1$ MV/cm.

molecular orientation degree is related to energy differences between neighboring rotational states [26]. The maximum orientation degree can be achieved at the instant when $|C_{J+1}(t)| \approx |C_J(t)|$. Under the continuous irradiation of a single-cycle THz laser pulse train, some $J \geq 2$ states can be excited and populated. When the rotational populations of neighboring states become nearly equal, the maximum orientation degree can be obtained. When the electric-field amplitude of THz laser pulse varies in the range of $E_0 = [0.1,1.2]$ MV/cm, a THz pulse train with $N \leq 20$ is an efficient way to enhance orientation degree.

We now discuss the variations of $|\langle\cos\theta\rangle|_{\max}$ with pulse number when $E_0>1.2$ MV/cm. It can be seen from Fig. 3(a) that the maximum orientation degree increases up to its extreme value, then begins to decrease with adding pulse number. There is an optimal pulse number for $E_0>1.2$ MV/cm to obtain the strongest molecular orientation. Fig. 3(b) shows the rotational population distributions when $N=18$, 19 and 20 and $E_0=1.3$ MV/cm. With increasing pulse number from $N=18$ to 20, the populations on the rotational states $|0,0\rangle$, $|1,0\rangle$, $|2,0\rangle$ and $|3,0\rangle$ decrease, while the populations on the $|4,0\rangle$, $|5,0\rangle$, $|6,0\rangle$ and $|7,0\rangle$ states increase. When $N=18$, 19 and 20, the maximum orientation degrees are $|\langle\cos\theta\rangle|_{\max}=0.9086$, 0.9127 and 0.9123, respectively. Thus the optimal pulse number for $E_0=1.3$ MV/cm is $N=19$. Fig. 3(c) shows the time evolutions of rotational populations

https://doi.org/10.4208/cicp.OA-2015-0001 Published online by Cambridge University Press

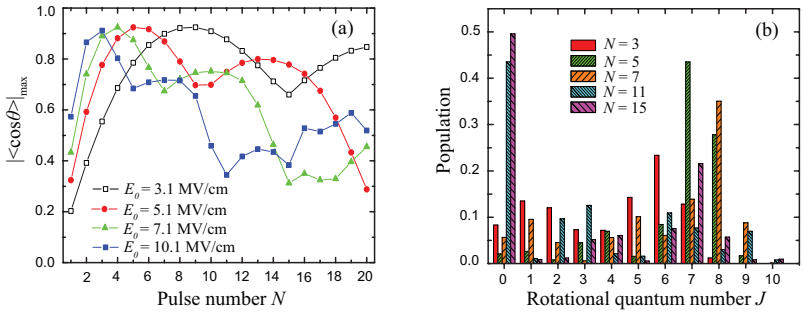


Figure 4: (a) The maximal orientation degree $|\langle\cos\theta\rangle|_{\max}$ as a function of the pulse number N for $E_0=3.1$ MV/cm (black open-square line), 5.1 MV/cm (red solid-circle line), 7.1 MV/cm (green solid-triangle line) and 10.1 MV/cm (blue solid-square line). (b) The rotational population distributions at $N=3$ (red bar), 5 (green bar), 7 (orange bar), 11 (cyan bar) and 15 (magenta bar) for $E_0=10.1$ MV/cm.

on the $J=0$–8 states when $E_0=2.1$ MV/cm and $N=20$. Because of the continuous excitation of the single-cycle THz pulse train, more and more rotational states are populated. Since there is no electric field within the time interval between two neighboring pulses (here the time interval is equal to the delay time), the population distribution remains unchanged before the next pulse. Fig. 3(d) shows the final rotational population distributions for different pulse numbers. We can see from Fig. 3(a) that the maximum orientation degree is $|\langle\cos\theta\rangle|_{\max}=0.9205$ for $N=12$ and $|\langle\cos\theta\rangle|_{\max}=0.8654$ for $N=16$. As shown in Fig. 3(d), the neighboring rotational populations are nearly equal when $N=12$, while the population differences between the $J=4$ state and $J=5$ state, $J=6$ state and $J=7$ state are very large for $N=16$. Thus the optimal pulse number is $N=12$ for $E_0=2.1$ MV/cm. This is consistent with the result about the influence of rotational populations on molecular orientation given by Ref. [26].

When $E_0>2.1$ MV/cm, the variations of $|\langle\cos\theta\rangle|_{\max}$ with pulse number are shown in Fig. 4(a). At $E_0=10.1$ MV/cm, for instance, $|\langle\cos\theta\rangle|_{\max}$ oscillates irregularly with the increase of pulse number. The extreme value of orientation degree reaches $|\langle\cos\theta\rangle|_{\max}=0.9116$ when $N=3$. Fig. 4(b) shows the rotational population distributions for different pulse number at $E_0=10.1$ MV/cm. The optimal pulse number for $E_0=10.1$ MV/cm is $N=3$.

We also investigate the dependence of molecular orientation on the electric-field amplitude. Fig. 5(a) illustrates the molecular orientation degree versus the peak intensity of THz pulse for $N=1$, 2 and 3. The corresponding population distributions are shown in Fig. 5(b-d). When the peak intensity of THz pulse increases, the dipole interaction strengthens. There are more rotational states being populated with increasing peak intensity, just as seen in Fig. 5(b-c), leading to a continuous increase of $|\langle\cos\theta\rangle|_{\max}$ in Fig. 5(a) for $N=1$ and 2. When $N=3$, $|\langle\cos\theta\rangle|_{\max}$ initially increases from 0.02 to 0.9203 when the peak intensity varies from $E_0=0.1$ to 9.1 MV/cm, then decreases slowly when $E_0>9.1$ MV/cm. It results from a big population difference between the $J=5$ and $J=6$ states, as well as the $J=6$ and $J=7$ states. In Fig. 6(a), when $N\geq 4$, the variations of $|\langle\cos\theta\rangle|_{\max}$ with

https://doi.org/10.4208/cicp.OA-2015-0001 Published online by Cambridge University Press

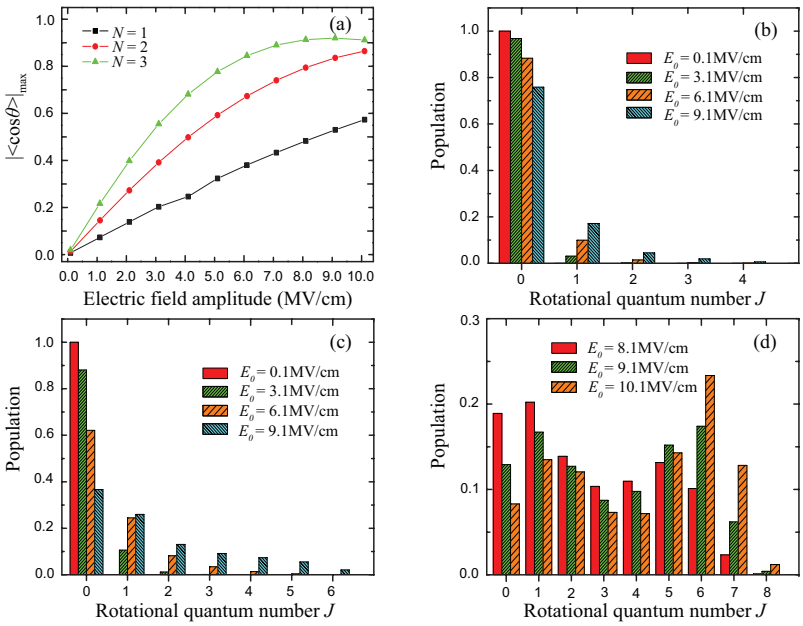


Figure 5: (a) The variation of $|\langle\cos\theta\rangle|_{\max}$ with the electric-field peak intensity E_0 for $N=1$ (black solid-square line), 2 (red solid-circle line) and 3 (green solid-triangle line). (b) The rotational population distributions at $E_0=0.1$ MV/cm (red bar), 3.1 MV/cm (green bar), 6.1 MV/cm (orange bar) and 9.1 MV/cm (cyan bar) for $N=1$. (c) The rotational population distributions at $E_0=0.1$ MV/cm (red bar), 3.1 MV/cm (green bar), 6.1 MV/cm (orange bar) and 9.1 MV/cm (cyan bar) for $N=2$. (d) The rotational population distributions at $E_0=8.1$ MV/cm (red bar), 9.1 MV/cm (green bar) and 10.1 MV/cm (orange bar) for $N=3$.

the peak intensity are very dramatic. When $N=20$, for instance, $|\langle\cos\theta\rangle|_{\max}$ increases from 0.1323 to 0.8977 when the peak intensity varies from $E_0=0.1$ to 1.1 MV/cm, then oscillates irregularly with the increase of peak intensity. The corresponding population distributions are shown in Fig. 6(b). Higher rotational states are populated by increasing the peak intensity, but the population difference of neighboring states enlarges at the same time. Accordingly, $|\langle\cos\theta\rangle|_{\max}$ decreases when $E_0>1.1$ MV/cm.

In the above calculations, we consider the orientation dynamics of the CO molecule at temperature $T=0$ K. In an actual experiment, however, the molecular ensemble is at finite temperature and more rotational states can be populated incoherently according to the temperature-dependent Boltzmann distribution. We take $N=14$ and $E_0=1.8$ MV/cm for example to study the effect of temperature on the maximum orientation degree. Fig. 7(a) shows the initial population distributions on the relevant rotational states at $T=0$, 10, 20, 30 and 40 K. The initial rotational population distributions varies with temperature, and higher rotational states are populated when temperature rises. The maximal orientation degree at $T=0$ K is $|\langle\cos\theta\rangle|_{\max}=0.9188$ which is much larger than 0.7338 at $T=10$ K, 0.6055 at $T=20$ K, 0.5154 at $T=30$ K and 0.4454 at $T=40$ K. Although the efficiency of orientation decreases with the increase of temperature, a larger orientation degree, $|\langle\cos\theta\rangle|_{\max}=0.5154$, is achieved at $T=30$ K.

https://doi.org/10.4208/cicp.OA-2015-0001 Published online by Cambridge University Press

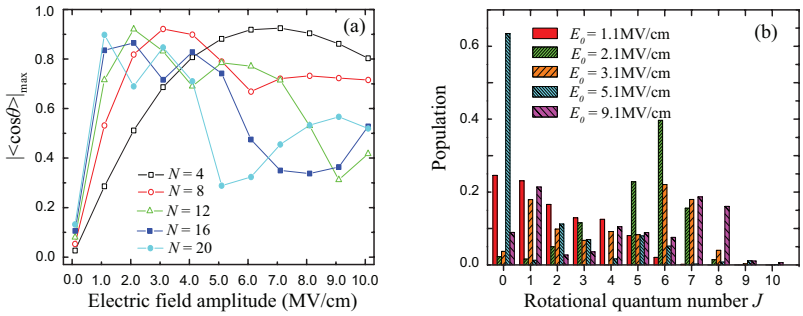


Figure 6: (a) The variation of $|\langle\cos\theta\rangle|_{\max}$ with the electric-field peak intensity E_0 for $N=4$ (black open-square line), 8 (red open-circle line), 12 (green open-triangle line), 16 (blue solid-square line)and 20 (cyan solid-circle line). (b) The rotational population distributions at $E_0=1.1$ MV/cm (red bar), 2.1 MV/cm (green bar), 3.1 MV/cm (orange bar), 5.1 (cyan bar) and 9.1 (magenta bar) for $N=20$.

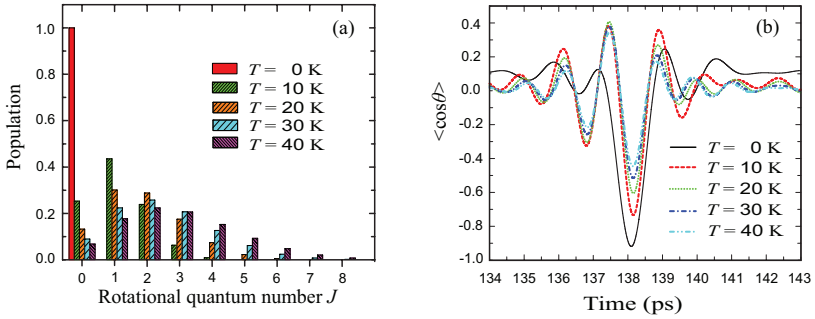


Figure 7: (a) The population distributions on rotational states at $T=0$ K (red bar), 10 K (green bar), 20 K (orange bar), 30 K (cyan bar) and 40 K (magenta bar). (b) The time evolution of the molecular orientation at $T=0$ K (solid line), 10 K (dash line), 20 K (dotted line), 30 K (dash dotted line) and 40 K (dash dotted dotted line), where $E_0=1.8$ MV/cm and $N=14$.

In many practical applications, such as the photoelectric effect and the electronically detecting process, one expects not only a high molecular orientation degree, but also a long duration time. The duration time of molecular orientation Δt is defined as the effective duration time that orientation degree ≥ 0.5. As shown in Fig. 7(b), the duration time of molecular orientation at $T=0$, 10, 20 and 30 K are $\Delta t=0.759$, 0.432, 0.297 and 0.117 ps in order. The relative duration time of molecular orientation at $T=0$, 10, 20 and 30 K are $\Delta t/\ T_{\mathrm{rot}}=8.78\%$, 5%, 3.44% and 1.35%, respectively.

4 Conclusions

We have investigated theoretically the molecular orientation steered by a single-cycle THz pulse train. We discuss the influence of pulse number and electric-field peak intensity on the field-free molecular orientation and find that the molecular orientation is closely associated with rotational population distribution. In the range of electric-field

https://doi.org/10.4208/cicp.OA-2015-0001 Published online by Cambridge University Press

peak intensity $E_0=[0.1,1.2]$ MV/cm, when the pulse number increases from $N=1$ to 20, more rotational states are excited, and the molecular orientation degree increases. When $E_0>1.2$ MV/cm, we can find an optimal pulse number to obtain the maximal orientation degree. By using the optimal pulse number, when the populations on neighboring rotational states are nearly equal, the molecular orientation degree takes its extreme value. When $E_0=10.1$ MV/cm, $|\langle\cos\theta\rangle|_{\max}$ oscillates irregularly with the increase of pulse number. The maximum orientation degree calculated is $|\langle\cos\theta\rangle|_{\max}=0.9246$. The optimal pulse number decreases with the increase of electric-field peak intensity. The optimal pulse numbers for $E_0=1.3$, 2.1 and 10.1 MV/cm are 19, 12 and 3, respectively. The temperature has drastic effect on molecular orientation. The molecular orientation degree decreases with the increase of temperature. The maximal field-free molecular orientation at $T=0$, 10, 20 and 30 K for $N=14$ and $E_0=1.8$ MV/cm are $|\langle\cos\theta\rangle|_{\max}=0.9188$, 0.7338, 0.6055 and 0.5154, respectively. The effective duration time of molecular orientation at $T=0$, 10, 20 and 30 K are $\Delta t=0.759$, 0.432, 0.297 and 0.117 ps in order. A high degree of molecular orientation and a long duration time can be realized by applying this scheme.

Acknowledgments

This work is supported by the National Natural Science Foundation of China under Grant Nos. 21473018 and 11374045.

References

[1] H. Stapelfeldt and T. Seideman, Colloquium: Aligning molecules with strong laser pulses, Rev. Mod. Phys., 75(2003) 543.
[2] H. Stapelfeldt and E. Hamilton, Nonadiabatic alignment by intense pulses. Concepts, theory, and directions, Adv. At. Mol. Opt. Phys., 52 (2005) 289-329.
[3] T. Kanai, S. Minemoto and H. Sakai, Quantum interference during high-order harmonic generation from aligned molecules, Nature, 435(2005) 470-474.
[4] T. Kanai, S. Minemoto and H. Sakai, Ellipticity dependence of high-order harmonic generation from aligned molecules, Phys. Rev. Lett., 98(2007) 053002.
[5] X.-B. Bian and A. D. Bandrauk, Orientation dependence of nonadiabatic molecular high-order-harmonic generation from resonant polar molecules, Phys. Rev. A, 86(2012) 053417.
[6] Y. Jin, X. Tong and N. Toshima, Anomalous alignment dependence of the third-order harmonic of H_2^+ ions in intense laser fields, Phys. Rev. A, 86(2012) 053418.
[7] C. Z. Bisgaard, O. J. Clarkin, G. Wu, A. M. D. Lee, O. Geßner, C. C. Hayden and A. Stolow, Time-Resolved Molecular Frame Dynamics of Fixed-in-Space CS_2 Molecules, Science, 323(2009) 1464-1468.
[8] F. Li, X.-Y. Hao and X.-G. Li, Efficient Grid Treatment of the Time Dependent Schrödinger Equation for Laser-Driven Molecular Dynamics, Commun. Comput. Phys., 13(2013) 1389-1407.
[9] J.-L. Li, Y. Huang, T. Xie, S. Chai and S.-L. Cong, Formation of NaH Molecules in the Lowest Rovibrational Level of the Ground Electronic State via Short-Range Photoassociation, Commun. Comput. Phys., 17(2015) 79-92.

https://doi.org/10.4208/cicp.OA-2015-0001 Published online by Cambridge University Press

[10] J. Hu, K.-L. Han and G.-Z. He, Correlation Quantum Dynamics between an Electron and D2+ Molecule with Attosecond Resolution. Phys. Rev. Lett., 95(2005) 123001.
[11] K.-J. Yuan, Z.-G. Sun, S.-L. Cong and N.-Q. Lou, Selective excitation of the OClO molecule with femtosecond laser pulse. Phys. Rev. A, 72(2005) 052513.
[12] I. V. Litvinyuk, K. F. Lee, P. W. Dooley, D. M. Rayner, D. M. Villeneuve and P. B. Corkum, Alignment-dependent strong field ionization of molecules, Phys. Rev. Lett., 90(2003) 233003.
[13] M. Lein, Molecular imaging using recolliding electrons, J. Phys. B, 40(2007) R135-R173.
[14] M. Meckel, D. Comtois, D. Zeidler, A. Staudte, D. Pavičić, H. C. Bandulet, H. Pépin, J. C. Kieffer, R. Dörner, D. M. Villeneuve, P. B. Corkum, Laser-Induced Electron Tunneling and Diffraction, Science 320(2008) 1478-1482.
[15] J. Küpper *et al*, X-Ray Diffraction from Isolated and Strongly Aligned Gas-Phase Molecules with a Free-Electron Laser, Phys. Rev. Lett., 112(2014) 083002.
[16] P.-F. Lan, P.-X. Lu, W. Cao, Y.-H. Li and X.-L. Wang, Carrier-envelope phase-stabilized attosecond pulses from asymmetric molecules, Phys. Rev. A, 76(2007) 021801(R).
[17] J. Chen, X. Cui, S. Zhou, B. Huang and X. Jiang, Numerical simulations of femtosecond-laser-induced dynamic alignment of molecules in the high-frequency off-resonance regime, Laser Phys., 12(2006) 1672-1680.
[18] G.-P. Zeng, F.-J. Zhong, C.-Y. Wu, H.-B. Jiang and Q.-H. Gong, Field-free molecular alignment and its application, Laser Phys., 19(2009) 1691.
[19] M. S. Molodenskiy and O. V. Tikhonova, Rotational dynamics of a molecular ensemble in the presence of a strong laser field, Laser Phys., 17(2007) 401.
[20] J. Wu, H. Cai, Y. Peng, Y.-Q. Tong, A. Couairon and H.-P. Zeng, Control of femtosecond filamentation by field-free revivals of molecular alignment, Laser Phys., 19(2009) 1759-1768.
[21] F. Rosca-Pruna and M. J. J. Vrakking, Experimental Observation of Revival Structures in Picosecond Laser-Induced Alignment of I_2, Phys. Rev. Lett., 87(2001) 153902.
[22] T. D. Hain, R. M. Moision and T. J. Curtiss, Hexapole state-selection and orientation of asymmetric top molecules: CH_2F_2, J. Chem. Phys., 111(1999) 6797.
[23] B. Friedrich and D. R. Herschbach, On the possibility of orienting rotationally cooled polar-molecules in an electric-field, Z. Phys. D, 18(1991) 153.
[24] B. Friedrich and D. Herschbach, Enhanced orientation of polar molecules by combined electrostatic and nonresonant induced dipole forces, J. Chem. Phys., 111(1999) 6157.
[25] B. Friedrich and D. Herschbach, Manipulating Molecules via Combined Static and Laser Fields, J. Phys. Chem. A, 103(1999) 10280.
[26] K. Kitano, N. Ishii and J. Itatani, High degree of molecular orientation by a combination of THz and femtosecond laser pulses, Phys. Rev. A, 84(2011) 053408.
[27] M. Machholm and N. E. Henriksen, Field-Free Orientation of Molecules, Phys. Rev. Lett., 87(2001) 193001.
[28] D. Daems, S. Guérin, D. Sugny and H. R. Jauslin, Efficient and Long-Lived Field-Free Orientation of Molecules by a Single Hybrid Short Pulse, Phys. Rev. lett., 94(2005) 153003.
[29] E. Gershnabel, I. S. Averbukh and R. J. Gordon, Enhanced molecular orientation induced by molecular antialignment, Phys. Rev. A, 74(2006) 053414.
[30] C.-C. Shu, K.-J. Yuan, W.-H. Hu and S.-L. Cong, Field-free molecular orientation with terahertz few-cycle pulses, J. Chem. Phys. 132(2010) 244311.
[31] C.-C. Qin, Y. Tang, Y.-M. Wang and B. Zhang, Field-free orientation of CO by a terahertz few-cycle pulse, Phys. Rev. A, 85(2012) 053415.
[32] T. Kanai and H. Sakai, Numerical simulations of molecular orientation using strong, non-resonant, two-color laser fields, J. Chem. Phys., 115(2001) 5492.

https://doi.org/10.4208/cicp.OA-2015-0001 Published online by Cambridge University Press

[33] S. De *et al*, Field-Free Orientation of CO Molecules by Femtosecond Two-Color Laser Fields, Phys. Rev. Lett., 103(2009) 153002.
[34] J. Wu and H. Zeng, Field-free molecular orientation control by two ultrashort dual-color laser pulses, Phys. Rev. A, 81(2010) 053401.
[35] M. Muramatsu, M. Hita, S. Minemoto and H. Sakai, Field-free molecular orientation by an intense nonresonant two-color laser field with a slow turn on and rapid turn off, Phys. Rev. A, 79(2009) 011403(R).
[36] Y. Liu, J. Li, J. Yu and S.-L. Cong, Field-free molecular orientation by two-color shaped laser pulse together with time-delayed THz laser pulse, Laser. Phys. Lett., 10(2013) 076001.
[37] S. Zhang, J. Shi, H. Zhang, T. Jia, Z. Wang and Z. Sun, Field-free molecular orientation by a multicolor laser field, Phys. Rev. A, 83(2011) 023416.
[38] Z.-M. Sheng, H.-C. Wu, W.-M. Wang, M. Chen, X.-G. Dong, J. Zheng and J. Zhang, Simulation of High Power THz Emission from Laser Interaction with Tenuous Plasma and Gas Targets†, Commun. Comput. Phys., 4(2008) 1258-1278.
[39] S. Fleischer, Y. Zhou, R. W. Field and K. A. Nelson, Molecular Orientation and Alignment by Intense Single-Cycle THz Pulses, Phys. Rev. Lett., 107(2011) 163603.
[40] C.-C. Shu and N. E. Henriksen, Field-free molecular orientation induced by single-cycle THz pulses: The role of resonance and quantum interference, Phys. Rev. A, 87(2013) 013408.
[41] Y. Huang, T. Xie, J. Li, J. Yu and S.-L. Cong, Efficiently field-free orientation of CO molecules by a femtosecond pulse and a THz pulse train, Laser Phys. 24(2014) 016002.
[42] S. Ramakrishna and T. Seideman, Intense Laser Alignment in Dissipative Media as a Route to Solvent Dynamics, Phys. Rev. Lett., 95(2005) 113001.
[43] S. Ramakrishna and T. Seideman, Disspative dynamics of laser induced nonadiabatic molecualr alignment, J. Chem. Phys., 124(2006) 034101.

https://doi.org/10.4208/cicp.OA-2015-0001 Published online by Cambridge University Press